A positional FEM Formulation for geometrical non-linear analysis of shells

Humberto Breves Coda* and Rodrigo Ribeiro Paccola

Universidade de São Paulo, Departamento de Engenharia de Estruturas,
São Carlos, São Paulo – Brazil

Abstract

This work presents a fully non-linear finite element formulation for shell analysis comprising linear strain variation along the thickness of the shell and geometrically exact description for curved triangular elements. The developed formulation assumes positions and generalized unconstrained vectors as the variables of the problem, not displacements and finite rotations. The full 3D Saint-Venant-Kirchhoff constitutive relation is adopted and, to avoid locking, the rate of thickness variation enhancement is introduced. As a consequence, the second Piola-Kirchhoff stress tensor and the Green strain measure are employed to derive the specific strain energy potential. Curved triangular elements with cubic approximation are adopted using simple notation. Selected numerical simulations illustrate and confirm the objectivity, accuracy, path independence and applicability of the proposed technique.

Keywords: Finite element method, geometrical non-linearity, large displacements, shell

1 Introduction

Following [19] one can say that a considerable number of nonlinear shell models which explicitly account for thickness change has been developed in the past years [2,7,13,14,17–20,22–24]. Most of these works incorporate the extra thickness strain terms at the element level via the enhanced assumed strain concept, leading very often to hybrid-mixed formulations. Some works like [17,18] provide only translational degrees-of-freedom in a continuum basis, but ill-conditioned systems are generated and additional locking effects appear. The purpose of this work is to present a new positional formulation for shell analysis that incorporates the rate of thickness variation directly in the kinematics and avoids the use of finite rotation schemes as Euler-Rodrigues formulae and similar [19,22]. As far as the authors' knowledge goes, the absence of finite rotations formulae and the positional characteristic of the shell formulation make it unique in literature. The second Piola-Kirchhoff stress tensor and the Green strain measure are employed to derive the formulation. Curved triangular elements with cubic approximation are developed. Selected numerical simulations illustrate and confirm the objectivity, accuracy, path independence and applicability of the proposed formulation.

2   Strain measure and specific strain energy potential

This section summarizes simple concepts used to derive the proposed formulation. The Green strain tensor is derived directly from the gradient of the change of configuration function (or deformation gradient), represented by letter A, given as follows:

$$A_{ij} = \frac{\partial f_i}{\partial x_j} \tag{1}$$

f_i is the change of configuration function, as depicted in figure 1, and ∂x_j represents variation regarding initial position. In figure 1 dx_i and dy_i represent an infinitesimal fiber in the initial and
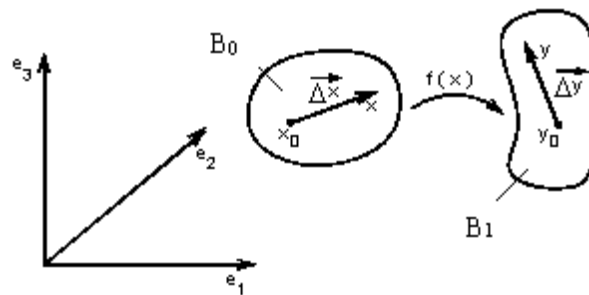

Figure 1: Change of configuration

current continuum configurations, respectively. Following [16], the Green strain can be written as:

$$E_{ij} = \frac{1}{2}\left[A_{ki}A_{kj} - \delta_{ij}\right] = \frac{1}{2}\left[C_{ij} - \delta_{ij}\right] \tag{2}$$

In which index notation is adopted. The variables C_{ij} and δ_{ij} are the right Cauchy-Green stretch tensor and the Kroenecker delta, respectively. The Saint-Venant-Kirchhoff strain energy per unit of initial volume is written as:

$$u_e = \frac{1}{2}E_{ij}C_{ijkl}E_{kl} \tag{3}$$

resulting in a linear elastic constitutive law relating second Piola Kirchhoff stress and Green strain, i.e.:

$$S_{ij} = \frac{\partial u_e}{\partial E_{ij}} = C_{ijkl}E_{kl} \tag{4a}$$

The elastic tensor is given by

$$C_{ijkl} = \frac{2G\nu}{1 - 2\nu}\delta_{ij}\delta_{kl} + G(\delta_{ik}\delta_{jl} + \delta_{il}\delta_{jk}) \tag{4b}$$

Where G is the shear modulus, given by,

$$G = \frac{E}{2(1+\nu)} \tag{4c}$$

with E being the well known Young modulus and ν the Poisson ratio. The relation among Second Piola Kirchhof stress and the true stress (Cauchy Stress) is straightforward [10, 16]. For the sake of completeness it is necessary to recall that the right Cauchy-Green stretch tensor is positive definite, symmetric and has six independent values [16].

3 Kinematical approximation and positional mapping

This section describes operational procedure to implement the proposed kinematics for shells taking into account the rate of thickness variation. It is important to note that expressions, simple as they are, are general and comprise curved elements. Appendix **A** is prepared specially to give a clear understanding of the unconstrained vector mapping, deriving it directly from a solid representation, conserving its capacity of describing what is called large rotations. If a solid has one of its dimensions smaller than others it is called a shell. One can approximate the mid-surface positions of a shell, see figure 2, by the following mapping.

$$f_i^{m0} = x_i^m(\xi_1, \xi_2, X_{\ell i}) = \phi_\ell(\xi_1, \xi_2) X_{\ell i} \tag{5}$$

$$f_i^{m1} = y_i^m(\xi_1, \xi_2, Y_{\ell i}) = \phi_\ell(\xi_1, \xi_2) Y_{\ell i} \tag{6}$$

where x_i^m is the ith coordinate of a generic point in the mid surface of the shell at initial configuration, $X_{\ell i}$ is the ith coordinate of node ℓ at initial configuration, y_i^m is the ith coordinate of a generic point in the mid surface of the shell at current configuration, $Y_{\ell i}$ is the ith coordinate of node ℓ at current configuration. A similar mapping has been proposed by [5] for membrane analysis. One can see in figure 2 that f^{m0} is the positional mapping from the auxiliary space to the initial configuration, f^{m1} is the positional mapping from the auxiliary space to the current configuration, f^m is the positional mapping from the initial configuration to the current one (not to be written) and the values A^{m0}, A^{m1}, A^m are their respective gradients. To complete the shell description for both initial and current configurations, one realizes that the difference among the coordinates of a point out of the mid-surface and its corresponding, belonging to the mid-surface, generates position vectors $\vec{g}^o$ or $\vec{g}^1$, see figure 3. By the other hand, a general point of the shell can be defined by adding the position vectors to the corresponding coordinates of a mid-surface point, i.e.,

$$x_i = x_i^m + g_i^0 \tag{7}$$

$$y_i = y_i^m + g_i^1 \tag{8}$$

For constant strain along thickness, following figure 3, one writes g_i^0 and g_i^1 as functions of non-dimensional variables, as

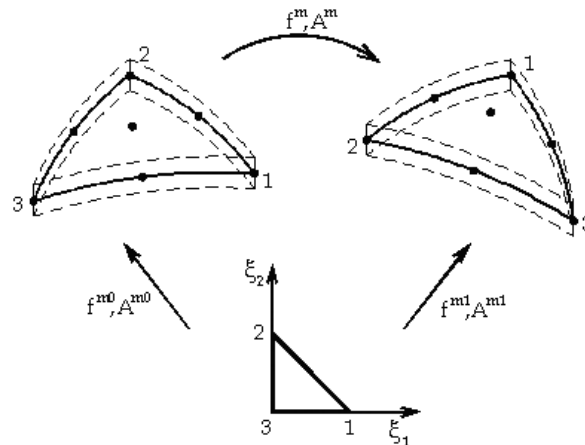$$g_i^0 = \frac{h_0}{2} e_i^0(\xi_1, \xi_2)\, \xi_3 \tag{9}$$

Figure 2: Mid-surface mapping

$$g_i^1 = \frac{h(\xi_1, \xi_2)}{2} e_i^1(\xi_1, \xi_2)\, \xi_3 \tag{10}$$

where h_0,h,e_i^0, e_i^1 are, respectively, the initial thickness of the shell, the current thickness of the shell, the normal unit vector to the initial mid-surface and the current unit vector, not normal to the current mid-surface. At this point it is important to mention that some classical formulations impose (at least at nodes) that e_i^1 is orthogonal to the mid surface and constraint to a spherical subspace governed by finite rotation variables, see for instance [3, 19, 21, 23]. It is also known that there are important formulations that consider the influence of shear strain in the kinematics and therefore the directors are not orthogonal to the final surface; see e.g. references [1,8,9]. As mentioned before, applying Reissner kinematics together with a complete 3D constitutive relation generates Poisson Locking, see for instance [4]. This problem is solved by considering an additional degree of freedom into the basic kinematics that considers linear strain along the thickness of the shell. To introduce this behavior, regarding ξ_3, a new scalar variable should be considered, it is called here the rate of thickness variation and is denoted by letter a. It is not necessary to introduce this new variable for initial configuration, so expression 9 does not change, however expression 10 turns into:

$$g_i^1 = \frac{h(\xi_1, \xi_2)}{2} e_i(\xi_1, \xi_2)\left[\xi_3 + a(\xi_1, \xi_2)\xi_3^2\right] \tag{11}$$

We will assume that the initial thickness is constant regarding the shell element and that e_i^0 is approximated as

$$e_i^0(\xi_1, \xi_2) = \phi_\ell(\xi_1, \xi_2) N_{i\ell}^0 \tag{12}$$

where $N_{i\ell}^0$ are normal unit vectors evaluated at nodal points ℓ for initial configuration. In expression 12 it is well known that the unitary norm of the initial normal vector is not preserved
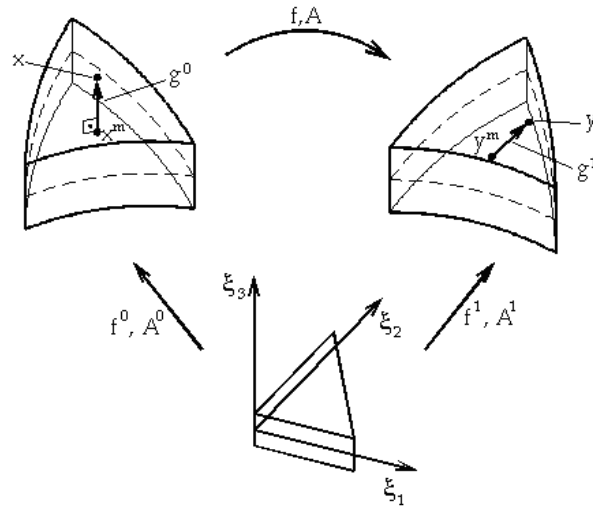
Figure 3: Position vectors and complete mapping

along the continuum element, see for instance [14]. This characteristic can be understood as an error in establishing the initial thickness of the shell. Using two and ten elements with cubic approximation (coarse and middle meshes) to model a $\pi/2$ cylindrical shell geometry, the maximum achieved error, for initial thickness, is 1.5% and 4.1 10^{-4}%, respectively. This result allows the use of this kind of approximation for practical purposes. Equations 13, 14 and 15 explain this concept when modeling the thickness of the current configuration. For the current configuration the following approximation is proposed,

$$h(\xi_1,\xi_2)e_i^1(\xi_1,\xi_2) = h_0\bar{g}_i(\xi_1,\xi_2) \tag{13}$$

where $\bar{g}_i$ is not a unit vector nor orthogonal to the mid surface, but the so-called generalized vector. From equation 13 one recovers the current thickness of the shell, varying over the element as

$$h(\xi_1,\xi_1) = h_0\sqrt{\bar{g}_i(\xi_1,\xi_1)\bar{g}_i(\xi_1,\xi_1)} \tag{14}$$

and the unit vector e_i as

$$e_i^1 = \frac{\bar{g}_i(\xi_1,\xi_1)}{\sqrt{\bar{g}_i(\xi_1,\xi_1)\bar{g}_i(\xi_1,\xi_1)}} \tag{15}$$

The position vectors, equations 9 and 11 are finally written as

$$g_i^0 = \frac{h_0}{2}\xi_3\phi_\ell(\xi_1,\xi_2)N_{i\ell}^0 \tag{16}$$

$$g_i^1 = \frac{h_0}{2}\left[\xi_3 + a(\xi_1,\xi_2)\xi_3^2\right]\phi_\ell(\xi_1,\xi_2)\bar{G}_{i\ell} \tag{17}$$

where $\bar{G}_{i\ell}$ are nodal values (unknown) of the generalized unconstrained vectors at node ℓ for current configuration. From these considerations equations 7 and 8 are rewritten as

$$f_i^0 = x_i = \phi_\ell(\xi_1, \xi_2) X_{\ell i} + \frac{h_0}{2} \xi_3 \phi_\ell(\xi_1, \xi_2) N_{i\ell}^0 \tag{18}$$

$$f_i^1 = y_i = \phi_\ell(\xi_1, \xi_2) Y_{\ell i} + \frac{h_0}{2} \left[\xi_3 + \phi_\ell(\xi_1, \xi_2) A_\ell \xi_3^2 \right] \phi_\ell(\xi_1, \xi_2) \bar{G}_{i\ell} \tag{19}$$

In which the rate of thickness variation (scalar) is parameterized by its nodal values A_ℓ, as follows:

$$a(\xi_1, \xi_2) = \phi_\ell(\xi_1, \xi_2) A_\ell \tag{20}$$

Equations 18 and 19 are the positional description of a solid with a dimension smaller than others, i.e., a shell. The unknown parameters per each node ℓ are seven, i.e., three positions $Y_{\ell i}$, three generalized nodal vectors $\bar{G}_{i\ell}$ and nodal rate of thickness variation A_ℓ. It is worth remembering that $\bar{G}_{i\ell}$ are not unitary nor orthogonal to the mid surface, i.e., $\bar{G}_{i\ell}$ are unconstrained and not related to finite rotation formulae. Function f_i^0 is used to find A^0 while function f_i^1 is used to find A^1 (trial). The composition of these two values for each integration station gives the numerical value of the gradient of the change of configuration for any initial geometry (curved), i.e., $A = A^1(A^0)^{-1}$. Forces are the energy conjugate of positions, therefore, it is possible to impose moments over nodes or faces using this formulation. One should realize that the conjugated of $\bar{G}_{i\ell}$ can change its modulus if and only if it has a component in its direction. Using this reasoning, to apply a moment over a node one uses a vector orthogonal to $\bar{G}_{i\ell}$ and the modulus of the moment is the modulus of this vector divided by the modulus of $\bar{G}_{i\ell}$. The last modulus is usually very near to the unity due to the high stiffness of the shell regarding the transverse direction. It is worth to show the derivatives of f_i^1 regarding non-dimensional variables, achieving the gradient A_{ij}^1 as follows:

$$A_{i1}^1 = \phi_{\ell,1}(\xi_1, \xi_2) Y_{\ell i} + \frac{h_0}{2} \left\{ \left[\xi_3 + \phi_\ell(\xi_1, \xi_2) A_\ell \xi_3^2 \right] \phi_{\ell,1}(\xi_1, \xi_2) \bar{G}_{i\ell} + \left[\phi_{\ell,1}(\xi_1, \xi_2) A_\ell \xi_3^2 \right] \phi_\ell(\xi_1, \xi_2) \bar{G}_{i\ell} \right\} \tag{21}$$

$$A_{i2}^1 = \phi_{\ell,2}(\xi_1, \xi_2) Y_{\ell i} + \frac{h_0}{2} \left\{ \left[\xi_3 + \phi_\ell(\xi_1, \xi_2) A_\ell \xi_3^2 \right] \phi_{\ell,2}(\xi_1, \xi_2) \bar{G}_{i\ell} + \left[\phi_{\ell,2}(\xi_1, \xi_2) A_\ell \xi_3^2 \right] \phi_\ell(\xi_1, \xi_2) \bar{G}_{i\ell} \right\} \tag{22}$$

$$A_{i3}^1 = \frac{h_0}{2} \left[1 + 2\phi_\ell(\xi_1, \xi_2) A_\ell \xi_3 \right] \phi_\ell(\xi_1, \xi_2) \bar{G}_{i\ell} \tag{23}$$

4   The numerical positional procedure

In this section the simplicity of the technique becomes clear, as no additional consideration is necessary. It is important to mention that parameters $X_{\ell i}$ and $N_{\ell i}^0$ are known quantities and will be called simply as $X_{\ell i}$ with i varying from one to six. The same is done for $Y_{\ell i}$, A_ℓ and $\bar{G}_{\ell i}$, i.e., the unknown quantities will be called simply by $Y_{\ell i}$ for i varying from one to seven. The

principle of minimum potential energy can be written, for a conservative elastostatic problem, using position considerations (not displacements) as follows:

$$\Pi(Y) = U_e(Y) - P(Y) \tag{24}$$

Where Π is the total potential energy, U_e is the strain energy and P is the potential energy of the applied forces, see figure 4. Assuming the strain energy per unity of initial volume as given
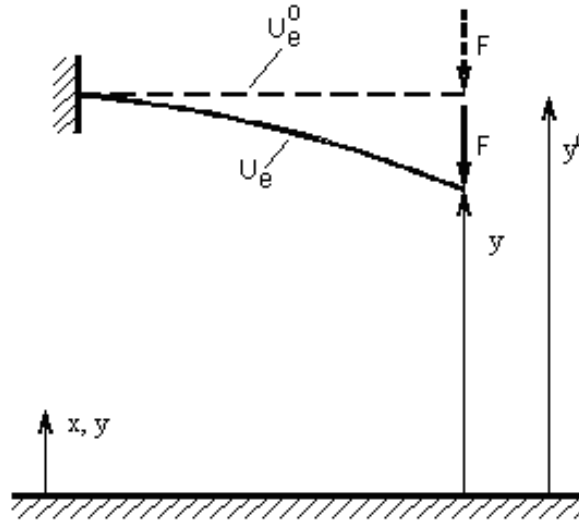

Figure 4: Total Potential Energy written for a body in two different positions.

by equation (3), recalling that the involved quantities are Lagrangian, the whole strain energy stored in the body is written for the reference volume V_0 as:

$$U_e = \int_{V_0} u_e \, dV_0 = \int_{V_0} \frac{1}{2} E_{kl} C_{klij} E_{ij} \, dV_0 \tag{25}$$

The potential energy of conservative applied forces is written as

$$P = Y_k F_k \tag{26}$$

In equation 26 Y_k corresponds to the current positions (not displacement), rate of thickness variation and generalized vectors at all points of the body, and F_k their corresponding forces. It is interesting to note that the potential energy of applied forces may not be zero in the reference configuration. From equations 25 and 26 the total potential energy is rewritten as

$$\Pi = \int_{V_0} \frac{1}{2} E_{kl} C_{klij} E_{ij} \, dV_0 - F_k Y_k \tag{27}$$

From the previous equations it is possible to write equation 27 as a function of current nodal positions and applied external forces. From this reasoning the problem of achieving the equilibrium of the elastic system is the determination of the minimum of total potential energy regarding positions. It is done by differentiating equation 27 regarding nodal positions and making it equal to zero. These steps are done as follows,

$$g_j = \frac{\partial \Pi}{\partial Y_j} = \int_{V_0} \frac{1}{2} \frac{\partial}{\partial Y_j} \left(E_{kl} C_{k\,\lim} E_{im}\right) dV_0 - F_j \qquad (28)$$

In equation 28 g_j is a vector that assumes null value for the exact position (solution). Splitting the derivative of the specific strain energy, one writes:

$$\frac{1}{2} \frac{\partial}{\partial Y_j} \left(E_{kl} C_{k\,\lim} E_{im}\right) = \frac{1}{2} \frac{\partial}{\partial E_{\alpha\beta}} \left(E_{kl} C_{k\,\lim} E_{im}\right) \frac{\partial E_{\alpha\beta}}{\partial Y_j} = C_{\alpha\beta im} E_{im} \frac{\partial E_{\alpha\beta}}{\partial Y_j} = \sigma_{\alpha\beta} \frac{\partial E_{\alpha\beta}}{\partial Y_j} \qquad (29)$$

Substituting equation 29 into equation 28 results

$$g_j = \int_{V_0} C_{\alpha\beta im} E_{im} \frac{\partial E_{\alpha\beta}}{\partial Y_j} dV_0 - F_j = F_j^{\text{int}} - F_j = 0 \qquad (30)$$

where F_j^{int} is the gradient vector of the strain energy potential regarding current positions, understood as internal force. Equation 30 means that if the internal force vector is equal to the applied one the solid is at equilibrium. If not, vector g_j can be understood as the unbalanced force of the mechanical system. It is important to remember that in this study the applied forces are conservative. Non-conservative forces can be introduced directly in equation 30, if desired. As mentioned before the nodal current positions are the unknown of the problem and, as a consequence, the solution of equation 30. As the vector function $g_j(E_{\alpha\beta}(Y_\ell))$ is non-linear regarding nodal parameters it is necessary to expand it from an initial trial solution, called here Y_ℓ^0, as follows:

$$g_j(Y_\ell) = g_j(Y_\ell^0) + \left.\frac{\partial g_j}{\partial Y_k}\right|_{(Y_\ell^0)} \Delta Y_k + O_j^2 = 0 \qquad (31)$$

Remembering that external forces are conservative one concludes that

$$\left.\frac{\partial g_j}{\partial Y_k}\right|_{(Y_\ell^0)} = \left.\frac{\partial F_j^{\text{int}}}{\partial Y_k}\right|_{(Y_\ell^0)} = \int_{V_0} \frac{\partial}{\partial Y_k} \left(C_{\alpha\beta im} E_{im} \frac{\partial E_{\alpha\beta}}{\partial Y_j}\right) dV_0 \Bigg|_{Y_\ell^0} = H_{kj}^0 \qquad (32)$$

where the matrix H_{kj}^0 is the complete Hessian matrix of the total potential energy. The derivative inside the integral term of equation (32) is written as:

$$\frac{\partial}{\partial Y_k} \left(C_{\alpha\beta im} E_{im} \frac{\partial E_{\alpha\beta}}{\partial Y_j}\right) = \left(\frac{\partial E_{im}}{\partial Y_k} C_{\alpha\beta im} \frac{\partial E_{\alpha\beta}}{\partial Y_j} + E_{im} C_{\alpha\beta im} \frac{\partial^2 E_{\alpha\beta}}{\partial Y_j \partial Y_k}\right) \qquad (33)$$

Neglecting higher order terms (O_i^2) equation 31 is rewritten as:

$$\Delta Y_k = -\left(H_{kj}^0\right)^{-1} g_j(Y_\ell^0) = \left(H_{kj}^0\right)^{-1}\left(F_j - F_j^{\text{int}}(Y_\ell^0)\right) \tag{34}$$

resulting into the full Newton-Raphson procedure to solve a non-linear system of equations. As the Hessian matrix is complete, the achieved Newton-Raphson procedure preserves the second order convergence rate. The Newton-Raphson procedure is summarized as follows: One chooses a trial position Y_ℓ^0 and calculates the unbalanced force vector $g_j(Y_\ell^0)$ according to equation 30. By applying equation 34 one finds the variation of position ΔY_k to correct Y_ℓ^0. With this new position vector, one repeats the procedure until ΔY_k or $g_j(Y_\ell^0)$ become small. The error, that is, the final unbalanced force (residuum) naturally considered by the next load step if the analyzed problem is divided into load steps, if not the problem is solved. To finalize the technique description the first and second derivatives of the Green strain regarding current nodal positions should be done. Firstly the necessary derivatives of the Cauchy-Green stretch tensor are presented. Next the derivatives of strains are straightforward achieved. Recalling that the Cauchy-Green stretch tensor is given by:

$$C = A^t A \tag{35}$$

and omitting, for simplicity, extra indices, one applies the positional FEM mapping and writes:

$$C = [(A^0)^t]^{-1}(A^1)^t(Y_i)A^1(Y_i)(A^0)^{-1} \tag{36}$$

Remembering that A_0 is constant regarding the current nodal position, the first derivative is performed as:

$$\frac{\partial C}{\partial Y_j} = [(A^0)^t]^{-1}\frac{\partial (A^1)^t(Y_i)}{\partial Y_j}A^1(Y_i)(A_0)^{-1} + [(A^0)^t]^{-1}(A^1)^t(Y_i)\frac{\partial A^1(Y_i)}{\partial Y_j}(A^0)^{-1}. \tag{37}$$

and, from equations 21 to 23, one has only 15 null values for the first derivatives regarding current positions and are left to the reader. Only terms relating generalized vectors and nodal rate of thickness variation will be present in the second derivative of A^1 regarding generalized positions. The general expression of the second derivative of the Cauchy-Green stretch is given by,

$$\begin{aligned}
\frac{\partial^2 C}{\partial Y_j \partial Y_k} =& [(A^0)^t]^{-1}\frac{\partial (A^1)^t(Y_i)}{\partial Y_j}\frac{\partial A^1(Y_i)}{\partial Y_k}(A^0)^{-1} + [(A^0)^t]^{-1}\frac{\partial (A^1)^t(Y_i)}{\partial Y_k}\frac{\partial A^1(Y_i)}{\partial Y_j}(A^0)^{-1} \\
&+ [(A^0)^t]^{-1}(A^1)^t(Y_i)\frac{\partial^2 A^1(Y_i)}{\partial Y_j \partial Y_k}(A^0)^{-1} + [(A^0)^t]^{-1}\frac{\partial^2 (A^1)^t(Y_i)}{\partial Y_j \partial Y_k}A^1(Y_i)(A^0)^{-1}
\end{aligned} \tag{38}$$

Recalling equation 2, one achieves directly the derivatives of Green strain regarding nodal positions, i.e.:

$$\frac{\partial E}{\partial Y_j} = \frac{1}{2}\frac{\partial C}{\partial Y_j} \qquad \frac{\partial^2 E}{\partial Y_j \partial Y_k} = \frac{1}{2}\frac{\partial^2 C}{\partial Y_j \partial Y_k} \tag{39}$$

It is important to mention that the present technique can be applied to any strain measure based on the Cauchy-Green stretch and any constitutive relation. Equations 30, 32 and 34 indicate that the proposed procedure can be operated by creating the Hessian matrix and internal forces for finite elements. Composing the global matrix and internal force vector is done by summation of coincident degrees of freedom, as in ordinary FEM procedures. One should remember that all nodal parameters follow the global system of reference, avoiding the use of rotation schemes.

5 Numerical examples

In a previous study [11] the positional formulation, using six parameters, was successfully tested using seven benchmark examples, mainly regarding its ability of representing large displacement situations using the engineering strain measure and linear constitutive relation; however a strong Poisson (volumetric) locking have been detected. The present formulation, including the seventh parameter $A\ell$ is proved to solve this limitation.

5.1 Thin plate bending - small displacement situation and locking analysis

This example is extracted from [6] and is used to check the formulation regarding Poisson and shear locking for thin shell undergoing small displacements. It is an important example as the solution for plates is very sensitive to the Poisson Ratio. It is the analysis of a simple supported square plate subjected to a transverse concentrated load at its center. The numerical results are compared to the analytical solution obtained using Navier's series and Kirchhoff plate theory. The thin plate geometry is depicted in figure 5.
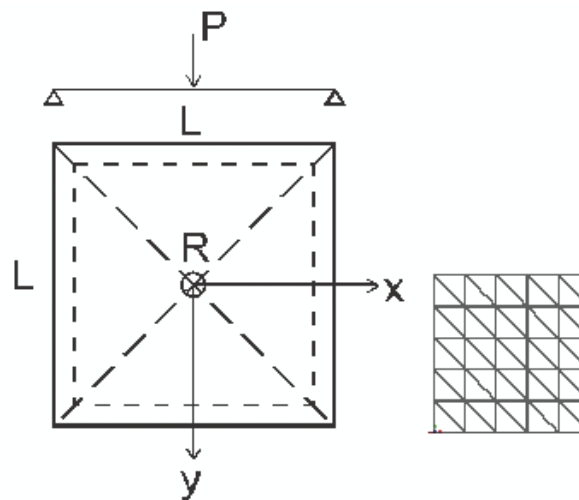

Figure 5: Analyzed plate and adopted discretization

The adopted physical properties are: $L = 2m$, $E = 2.1x10^6 kPa$, $h = 0.002m$ and v varying from 0 to 0.5. The applied load is $P = 0.4x10^{-2}N$. In figure 6 the results obtained using the positional formulation with six and seven parameters are compared to the analytical solution.
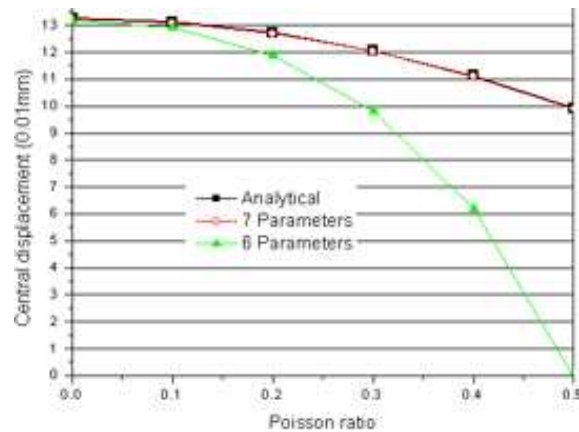

Figure 6: Displacement at the centre of the plate versus Poisson Ratio.

As one can observe the seven parameters positional formulation is free from locking and reproduces perfectly the analytical solution while the six parameter formulation locks totally.

5.2   Pinched cylinder with rigid diaphragms

A cylinder with rigid diaphragms is pinched by concentrated loads at two opposite points at its top and bottom, see figure 7. Two discretizations are adopted. The first, for the six parameter formulation, is a mesh of $2 \times 21 \times 8$ curved triangular finite elements resulting in 1600 nodes, 81 less than the number used by [23]. The second is a coarser mesh, $2 \times 18 \times 6$, 1045 nodes, for the consideration of the seventh parameter. The adopted discretization for seven parameters is shown at figure 7. Taking advantage of symmetry only one octant of the cylinder is discretized. The adopted physical properties are: $R = 100$, $h = 1$, $E = 3x10^4$, $L = 200$. Two values are adopted for the Poisson ratio, $v = 0.3$ and $v = 0.49$, respectively, in order to check the locking free behavior of the present formulation.

In figure 8 the results for $v = 0.3$ are compared with the one presented by [23] that employed an enhanced quadrilateral strain based shell finite element. As one can see the positional seven parameter formulation, presented here, can capture the flexibility of the pinched shell even for this coarse mesh.

In figure 9, the behavior of the six and seven parameters positional formulation are compared for $v = 0.49$. The reference value for this figure is the seven parameter formulation with $v = 0.3$. As expected, the seven parameter formulation does not lock for large Poisson ratio while the results for six parameters lock completely.
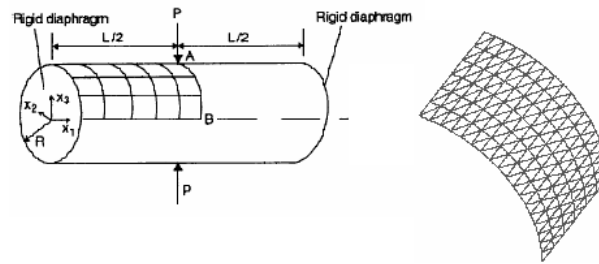
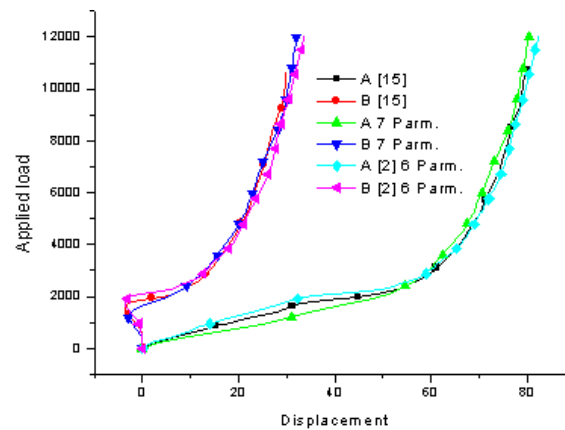Figure 7: Pinched Cylinder geometry, loading and six parameter discretization.

Figure 8: Displacements for points A and B, $\upsilon = 0.3$.

From the results it is obvious that the positional seven parameters formulation together with high order curved elements is able to solve geometrically non-linear shell problems with precision and reduced mesh. Moreover, the introduction of the seventh parameter results in a locking free behavior. Additional information is that the pinched cylinder benchmark problem is not very sensitive to the Poisson ratio intensity, when a locking free formulation is employed.

5.3   Objectivity of the formulation regarding rotations

As mentioned in the introduction, this formulation is tested regarding mapping objectivity and path dependence. The employed way to test this property follows well known methodologies, see for instance [12,15]. A clamped vertical plate (shell in deformed configuration) is subject to a transverse load at its free end as depicted in figure 10. The physical properties of the structure are $E = 100000$ and $\nu = 0$. The thickness of the shell is $h = 0.1$. The adopted discretization is shown in figure 10.

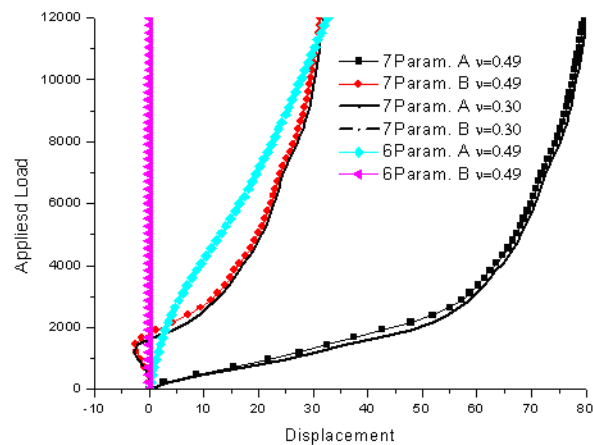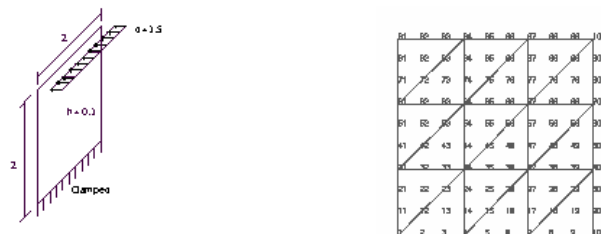Two situations are created. The first consists in applying a rotation of the clamped end

Figure 9: Displacements for points A and B, $\upsilon = 0.49$.

Figure 10: Geometrical characteristics of the problem and discretization.

regarding the clamping axis without applying any load. The objective is to show that no stress will be generated at any stage of rotation. One hundred turns are applied and no stress appears; moreover the positions are exactly the same after each turn. In figure 11 one can see an illustration of this situation for the first turn. The adopted rotation step is 0.1π.

In the second situation the process is divided into two phases and both objectivity and path dependence are tested. First, the load is increased to its final value in ten equal steps. The resulting stress, following the longitudinal direction of the shell, at the superior face of the shell, is depicted in figure 12.

Then the load is kept constant and acting in the same sense and direction and the rotation, similar to the one used in the first situation, is applied. The adopted rotation step is 0.01π. At the beginning of the rotation process the action of rotation is against the action of the loading. At a quarter of the first turn the loading is compressing the shell and the stress values, following the longitudinal direction of the shell, are depicted in figure 13.

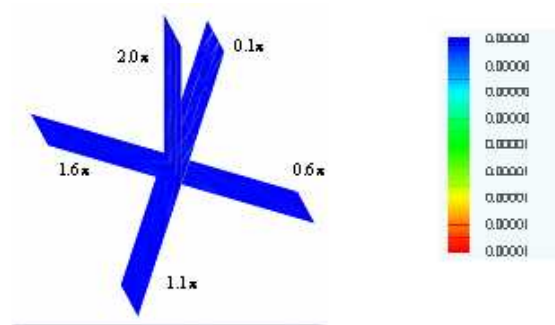At the half of the first turn the shell is in opposite position to the beginning of the rotation

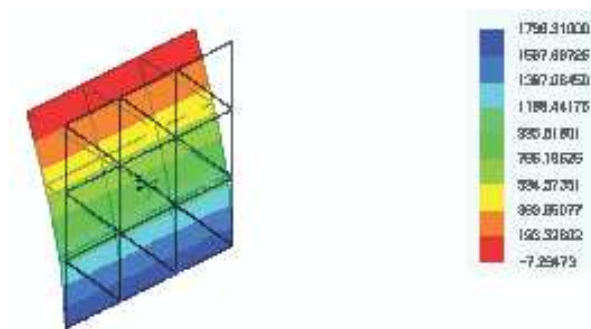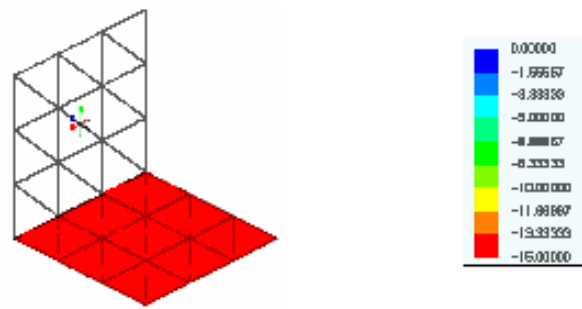Figure 11: Stress values for the first turn -unloaded

Figure 12: Stress values for the first deformed configuration - no rotation

process, and the initially superior face of the shell is now the inferior one. The stress values at this face are negative and their values are depicted in figure 14. The difference in stress magnitude from the first deformed configuration and this one is due to the normal traction force that increases the values in figure 12 and decreases the absolute values in figure 14.

At three quarters of the first turn the stress values are the ones depicted in figure 15, exactly as expected.

Finally, after a complete revolution the stress values depicted in figure 12 are exactly recovered. Ninety nine more turns were performed and the results are repeated for each turn, revealing the total objectivity of the generalized vector mapping.

After 100 turns the load is reduced to zero and the no-stress situation and displacement is achieved, revealing the path independence of the formulation. It is worth noting that [12] demonstrated mathematically the path dependence of finite rotation descriptions.

Figure 13: Stress values for a quarter of the first turn ($\pi/2$)
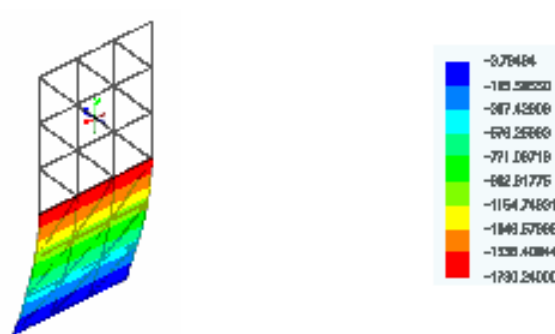
Figure 14: Stress values for the half turn (π)

6 Conclusions

In the present work a non-conventional way to derive finite element formulation for shell analysis is presented including the rate of thickness variation in the positional formulation. The novelty of positional formulation is the consideration of positions and generalized unconstrained vectors as nodal parameters, not displacements and finite rotations. This feature allows an easy development of curved high order elements. Moreover, the resulting formulation is path independent and objective as demonstrated by examples. The formulation has been described and implemented for triangular curved shell elements with cubic approximation for positions, generalized vectors and rate of thickness variation, using simple language and notation. Results are in very good agreement with the ones present in specialized literature. As expected, the seventh parameter guarantees a locking free behavior, as demonstrated by the first two examples, and no simplification is required in the constitutive relation. Future developments are the consideration of rubber like materials, dynamics and plasticity.
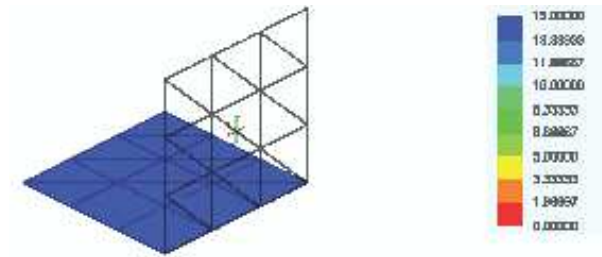
Figure 15: Stress values for three quarters of a turn $(3\pi/2)$

Appendix A - Basic unconstrained mapping

In this appendix the standard FEM solid mapping is transformed to an unconstrained vector mapping in order to help in the understanding of section 3. Figure A1 shows, without loss of generality, a two-dimensional solid element, with quadrangular form, mapped from the non-dimensional Gauss' space to its shape, following the classical procedure and the vector procedure.
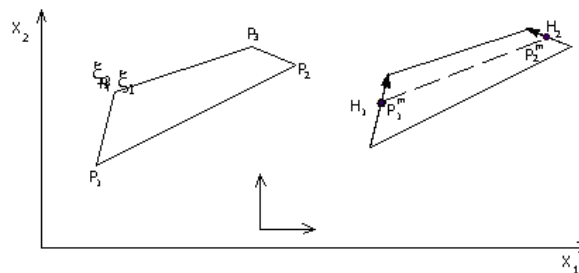

Figure A1: Solid element, classical and vector mapping.

Firstly, the transformation is shown for a two-dimensional solid element with a low order approximation. After that it is generalized for the desired shell element. The adopted low order shape functions are:

$$\phi_1(\xi_1, \xi_2) = \frac{1}{4}\left(1 - \xi_1\right)\left(1 - \xi_2\right) \tag{A1}$$

$$\phi_2(\xi_1, \xi_2) = \frac{1}{4}\left(1 + \xi_1\right)\left(1 - \xi_2\right) \tag{A2}$$

$$\phi_3(\xi_1, \xi_2) = \frac{1}{4}\left(1 + \xi_1\right)\left(1 + \xi_2\right) \tag{A3}$$

$$\phi_4(\xi_1, \xi_2) = \frac{1}{4}\left(1 - \xi_1\right)\left(1 + \xi_2\right) \tag{A4}$$

And for the vector discretization the longitudinal shape functions are:

$$\varphi_1(\xi_1) = \frac{1}{2}\left(1 - \xi_1\right). \tag{A5}$$

$$\varphi_2(\xi_1) = \frac{1}{2}(1 + \xi_1) \tag{A6}$$

where ξ_i are non-dimensional Gauss' coordinates, see figure A1. The classical mapping is written as:

$$x_i(\xi_1, \xi_2, X_{\ell i}) = \phi_\ell(\xi_1, \xi_2)X_{\ell i} \text{ for } i = 1, 2 \text{ and } \ell = 1, 2, 3, 4 \tag{A7}$$

where x_i are any coordinates of a continuum point, $\phi_\ell(\xi_1, \xi_2)$ are the shape functions and $X_{\ell i}$ are the coordinates of nodes P_ℓ, called nodal position parameters. The equivalent vector mapping, related to equation A7, is achieved making very simple algebraic operations and is given as:

$$x_i(\xi_1, \xi_2, X_{\ell i}^m, V_{\ell i}) = \varphi_\ell(\xi_1)X_{\ell i}^m + \frac{H_{\ell i}\varphi_\ell(\xi_1)}{2}\xi_2 \text{ for } i = 1, 2 \text{ and } \ell = 1, 2 \tag{A8}$$

Where the nodal coordinates of the reference line $X_{\ell i}^m$ and the generalized vectors $H_{\ell i}$ are given by:

$$X_{1i}^m = \frac{X_{1i} + X_{4i}}{2}; \ X_{2i}^m = \frac{X_{2i} + X_{3i}}{2}; \ H_{1i} = X_{4i} - X_{1i} \text{ and } H_{2i} = X_{3i} - X_{2i} \tag{A9}$$

Expression A8 shows that the vector mapping is done using non-unitary vectors $H_{\ell i}$ as parameters. Moreover, these vectors are not orthogonal to the reference line. To generalize this procedure, one writes the nodal vectors H_{1i} and H_{2i} as functions of heights H_1 and H_2, finding:

$$x_i(\xi_1, \xi_2, X_{\ell i}^m, V_{\ell i}, H_\ell) = \varphi_\ell(\xi_1)X_{\ell i}^m + \frac{H_{(\ell)}}{2}\xi_2 V_{i\ell}\varphi_\ell(\xi_1) \text{ for } i = 1, 2 \text{ and } \ell = 1, 2 \tag{A10}$$

Index inside brackets accompany sum, but does not mean summation. The first term of equation A10 describes the reference line approximation and can be easily enhanced. The values $V_{i\ell}$ are the generalized vectors. Their approximation, along the length of the bar, is also easily enhanced, as will be shown in the next section. These vectors are not orthogonal to the reference line and may not be of unit value, if desired, see equation A8. Regarding the initial configuration of the analyzed body, for simplicity, the generalized vectors are chosen unitary and orthogonal to the reference line, however for the current configuration of the body they are not. This is the main characterisitic of the unconstrained vector mapping. Finally, one assumes, as usual, constant height (h_0) for frame elements and equation A10 is transformed into the desired mapping:

$$x_i(\xi_1, \xi_2, X_{\ell i}^m, V_{\ell i}) = \varphi_\ell(\xi_1)X_{\ell i}^m + \frac{h_0}{2}\xi_2 V_{i\ell}\varphi_\ell(\xi_1) \text{ for } i = 1, 2 \text{ and } \ell = 1, 2 \tag{A11}$$

It is straightforward to transform equation A11 into a shell representations, one needs only to substitute the mid line approximation by a mid surface approximation, i.e.:

$$x_i(\xi_1, \xi_2, \xi_3, X_{\ell i}^m, V_{\ell i}) = \phi_\ell(\xi_1, \xi_2)X_{\ell i}^m + \frac{h_0}{2}\xi_3 V_{i\ell}\phi_\ell(\xi_1.\xi_2) \tag{A12}$$

This expression is exactly the same as the equation 18 of the maim text. In the main text, vector $V_{i\ell}$ is called $N_{i\ell}^0$ for initial configuration and $\bar{G}_{i\ell}$ for current configuration. Moreover an enhancement of transverse strain is proposed there for the seven parameter formulation. As equation A12 is a solid description, as equation A7, it is able to comprise any movement of the body, including the so called finite rotations.

References

[1] KJ. Bathe and EN. Dvorkin. A formulation of general shell elements-the use of mixed interpolation of tensorial components. *International Journal for Numerical Methods in Engineering*, 22:697–722, 1986.

[2] P. Betsch, F. Gruttmann, and E. Stein. A 4-node finite shell element for the implementation of general hyperelastic 3delasticity at finite strains. *Comput. Meth. Appl. Mech. Engrg.*, 130:57–79, 1996.

[3] P. Betsch and P. Steinmann. "constrained dynamics of geometrically exact beams". *Computational Mechanics*, 31:49–59, 2003.

[4] M. Bischoff and E. Ramm. On the physical significance of higher order kinematic and static variables in a three-dimensional shell formulation. *International Journal of Solids and Structures*, 37(46-47):6933–6960, P.G.2000.

[5] J. Bonet, R. D. Wood, J. Mahaney, and P. Heywood. "finite element analysis of air supported membrane structures". *Computer Methods in Applied Mechanics and Engineering*, 190(5-7):579–595, 2000.

[6] M.L. Bucalem and S.H.S. Nóbrega. A mixed formulation for general triangular isoparametric shell elements based on the degenerated solid approach. *Computers and Structures*, 78:35–44, 2000.

[7] N. Büchter, E. Ramm, and D. Roehl. Three-dimensional extension of nonlinear shell formulation based on the enhanced assumed strain concept. *Int. J. Numer. Meth. Engrg.*, 37:2551–2568, 1994.

[8] D. Chapelle and KJ. Bathe. *The Finite Element Analysis of Shells: Fundamentals*. Springer, 1 edition 2003.

[9] D. Chapelle and KJ. Bathe. The mathematical shell model underlying general shell elements. *International Journal for Numerical Methods in Engineering*, 48:289 –313, 2000.

[10] P.G. CIARLET. *Mathematical Elasticity*. North Holland, 1993.

[11] H.B. Coda and R.R Paccola. An alternative positional fem formulation for geometrically non-linear analysis of shells - curved triangular isoparametric elements. *Computational Mechanics*, 40(1):185–200, 2007.

[12] M. A. Crisfield and G. Jelenic. "objectivity of strain measures in the geometrically exact three-dimensional beam theory and its finite element implementation". *Proc. R. Soc. Lond.*, A 455:1125–1147, 1999.

[13] R.J.A. de Sousa, R.P.R. Cardoso, and R.A.F Valente. A new one-point quadrature enhanced assumed strain (eas) solid-shell element with multiple integration points along thickness - part ii: Nonlinear applications. *International Journal for Numerical Methods in Engineering*, 67 (2):160–188, 2006.

[14] N. El-Abbasi and S.A. Meguid. A new shell element accounting for through-thickness deformation. *Comput. Meth. Appl. Mech. Engrg.*, 189:841–862, 2000.

[15] A. Ibrahimbegovic and R. L. Taylor. "on the role of frame-invariance in structural mechanics models at finite rotations". *Comput. Methods Appl. Mech. Engrg.*, 191:5159–5176, 2002.

[16] R.W. OGDEN. *Non-linear Elastic deformation*. Ellis Horwood, England, 1984.

[17] H. Parisch. A continuum-based shell theory for nonlinear applications. *Int. J. Numer. Meth. Engrg.*, 38:1855–1883, 1995.

[18] A. Petchsasithon and P.D. Gosling. A locking free hexahedral element for the geometrically non-linear analysis of arbitraryshells. *Computational Mechanics*, 35:94–114, 2005.

[19] P.M. Pimenta, E.M.B, Campello, and P. Wriggers. A fully nonlinear multi-parameter shell model with thickness variation and a triangular shell finite element. *Computational Mechanics*, 34:181–193, 2004.

[20] P. Wriggers R. Eberlein. Finite element concepts for finite elastoplastic strains and isotropic stress response inshells: Theoretical and computational analysis. *Comput. Meth. Appl. Mech. Engrg.*, 171:243–279, 1999.

[21] I. Romero and F. Armero. "an objective finite element approximation of the kinematics of geometrically exact rods and its use in the formulation of an energy-momentum conserving scheme in dynamics". *International Journal for Numerical Methods in Engineering*, 54(12):1683–1716, 2002.

[22] C. Sansour. A theory and finite element formulation of shells at finite deformations including thickness change: Circumventing the use of a rotation tensor. *Arch. Appl. Mech.*, 65:194–216, 1995.

[23] C. Sansour and F.G. Kollmann. Families of 4-node and 9-node finite elements for a finite deformation shell theory. anassessment of hybrid stress, hybrid strain and enhancedstrain elements. *Comput. Mech.*, 24:435–447, 2000.

[24] J.C. Simo, M.S. Rifai, and D.D. Fox. On a stress resultant geometrically exact shell model. part iv: variable thickness shells with through-the-thickness stretching. *Comput. Meth. Appl. Mech. Engrg.*, 81:91–126, 1990.